PREDICTION OF ULTIMATE LOAD OF CONCRETE BEAMS REINFORCED WITH FRP BARS USING ARTIFICIAL NEURAL NETWORKS

Ahmed Sagban Saadoon, Basrah Univ., Civil Eng. Dept., ahmsag@gmail.com
Hawraa Sami Malik Basrah Univ., Civil Eng. Dept., wesamsalm85@gmail.com
Received on 09 October 2016 Accepted on 22 December 2016

Abstract

Artificial neural networks (ANN) were used in this study to predict ultimate load of simply supported concrete beams reinforced with FRP bars under four point loading. A proposed neural model was used to predict the ultimate load of these beams. A total number of (199) beams (samples) were collected as data set and it was decided to use eight input variables, representing the dimensions of beams and properties of concrete and FRP bars, while the output variable was only the ultimate load of these beams. It was found that the use of 11 and 10 nodes in the two hidden layers was very efficient for predicting the ultimate load. The obtained results were compared with available experimental results and with the ACI 440.1R specifications. The proposed neural model gave very good predictions and more accurate results than the ACI 440.1R approach. The overall average error, in the value of the predicted ultimate load, was 3.6% and 21.7% for the proposed neural model and the ACI 440.1R approach, respectively.

Key words: FRP bars, flexural behavior, artificial neural networks.

تقدير الحمل الأقصى للعتبات الخرسانيّة المسلّحة بقضبان بوليميريّة باستخدام الشبكات العصبيّة الاصطناعيّة

احمد صكبان سعدون, قسم الهندسة المدنية, جامعة البصرة، العراق، ahmsag@gmail.com

حوراء سامي مالك, قسم الهندسة المدنية, جامعة البصرة, العراق، wesamsalm85@gmail.com

الخلاصة

لقد تمّ استخدام الشبكات العصبيّة الاصطناعيّة في هذه الدراسة لتقدير الحمل الأقصى للعتبات الخرسانيّة بسيطة الإسناد والمسلحّة بقضبان تسليح بوليميريّة والمعرّضة الى تحميل نقطي رباعي. حيث تمّ إقتراح وتطوير شبكة عصبيّة لتقدير الحمل الأقصى لهذه العتبات وقد جُمعت نتائج (١٩٩) نموذج كقاعدة بيانات. وقد تقرّر أنْ يكون عدد متغيّرات الإدخال لهذه الشبكة هو ثمان متغيّرات تمثّل أبعاد العتبات وخواص الخرسانة وقضبان التسليح، في حين كان هناك متغيّراً وحيداً هو الحمل الأقصى كمتغيّر إخراج. لقد وُجد بأنّ اختيار ١١ عقدة (خليّة عصبيّة) في الطبقة المخفيّة الاولى من الشبكة و ١٠ عقد في الطبقة الثانية كان فعّالاً جدّاً في تقدير قيمة الحمل الأقصى. وقد قُورنت النتائج المستحصلة مع نتائج عمليّة متوفّرة ومع مواصفات المدوّنة الأمريكيّة ACI 440.1R حيث أعطت الشبكة المقترحة نتائج أكثر دقّة من المدوّنة الأمريكيّة، إذ كان مقدار معدّل الخطأ الكلّي في قيمة الحمل الأقصى المقدّر هو ٣.٦% باستخدام الشبكة المقترحة بينما كان مقداره ٢١.٧% باستخدام المدوّنة الأمريكيّة.

Nomenclature

a	Shear span (mm)
a	Summation function
A_f	Area of FRP bar (mm^2)

ACI	American Concrete Institute
ANN	Artificial neural network
b	Width of beam (mm) or bias
E_f	FRP elasticity modulus (MPa)
f	Activation function
f'_c	Compressive strength of concrete (MPa)
f_u	FRP tensile strength (MPa)
FOV	Fraction of variance
FRP	Fiber reinforcement polymer
h	Beam's depth (mm)
L	Beam's length (mm)
Logsic	Logistic sigmoidal function
m	Shear span ratio (a/L)
MAE	Mean absolute error
MAPE	Mean absolute percentage error
MSE	Mean square error
N	Number of input samples (vectors)
P	Ultimate load (kN)
P_{ACI}	Ultimate load predicated by ACI code (kN)
P_{ANN}	Ultimate load predicated by neural network (kN)
P_{exp}	Experimental ultimate load (kN)
Purelin	Linear function
R	Coefficient of correlation
RMSE	Root mean squared error
tansig	Hyperbolic tangent function
u	Actual value
v	Predicted value
$\overline{u}$	Mean of the actual values
w	Weight vector
x	Neural input
y	Neural output

1 General

The ultimate strength in reinforcing members is depending on the type of reinforcement materials. Due to durability and corrosion problem of steel reinforcement under aggressive conditions, other materials, like fiber reinforcement polymers (FRP), have appeared to be an alternative reinforcement material. The FRP reinforcing bars are a composite materials made of reinforcing fibers and a matrix (resin). FRP composites are used in many types of engineering structures and can be used for enhancing requirements of performance due to their advantageous properties. FRP composites are utilized in rehabilitation, formwork, and reinforcement for seismic design [Jain and lee, 2012].

FRP reinforced concrete members started to be used all over the world, specifically in areas like flexural behavior, bond performance, column behavior and shear behavior. In structural applications, FRP are available as plates, strips or sheets, and reinforcing bars. The use of FRP can be either as an alternative reinforcing instead of steel or for retrofitting to strengthening existing structures. FRP are used as internal or external reinforcement to strengthen columns, slabs, and beams. The strength of these members can be increased even after their damage due to subjected loading.

Many experimental and theoretical investigations [6, 11, 15, 18, and 29] were performed to study the structural and flexural behavior of FRP reinforced concrete beams. These beams are expected to undergo larger deformations than corresponding steel reinforced beams, since the modulus of elasticity of FRP bars is low. FRP bars have high ultimate strength and a linear stress-strain response. This would lead to an almost linear load-deflection response beyond the crack formation phase, up to failure. In this study, an attempt is made to get and predict the ultimate load of FRP reinforced concrete beams using artificial neural networks.

2 Artificial Neural Networks (Ann)

ANNs are computational networks which simulating a biological neural network. Due to this, they allow using simple and basic operations to solve nonlinear or complex problems [Graupe, 2007]. Neural networks are considered good for regression and classification tasks in practical cases [Begg et al., 2006]. This makes ANN a very efficient tool to solve and deal with many structural and civil engineering problems [see 21, 24, and 31], particularly in problems having complex or insufficient data.

Basically, all ANNs have the same structure or topology, the most common arrangement of the neurons by using a series of layers as shown in **Figure (1)**. The first layer is the layer of input. The input units at this layer is dictated by the number of independent variables or feature values and the input data are taken either directly from electronic sensors or from input files. The final layer is

the output layer which its units depend on the number of values or classes to be predicated and it sends information to the outside world or other devices like a mechanical control system, or a secondary computer system. The intermediate layers are called the hidden layers which contain many neurons in different interconnection structures. **Figure (2)** shows the scheme of a model of an artificial neuron. The shown model has N number of input and one output. The body of neuron contains the summing junction ($\sum$) and the activation function f. The following parameters and variables are used in the artificial neurons.

Every input has its own weight, which gives it the effect that it requires to process elements summation function. The node's internal bias (b) is a constant component represents the magnitude offset that affects the activation of the node output. The input vector and the weights vector can be represented as ($x_1, x_2, ..., x_N$) and ($w_1, w_2, ……, w_N$), respectively. The summation function can be calculated by multiplying of vector x and w and then adding up the products:

$$a = \sum_{i=1}^{N} (w_i x_i) + b \quad , \qquad (1)$$

The result will be as a single number. This weighted sum, from summation function, is transformed to the working output though an algorithmic process called transfer function. When neurons are sufficiently activated its output will take a value of 1, but it take zero when the neuron is not sufficiently activated. There are many activation functions used in neural networks which specify the neuron output to a given input.

3 Development Of Proposed Neural Model

An artificial neural model is proposed to predict the ultimate load of simply supported FRP reinforced concrete beams under four point loading as shown in **Figure (3)**. The neural network program that is implemented in MATLAB version 8.3.0.532 (R2014a) is used for performing the neural network in this study. This program has many advantages such as containing several types of networks and implementing many different training algorithms.

Back-propagation neural networks are proposed to study the relations between the input variables and the output variables by using the feed-forward back-propagation algorithm. The trial and error process is used to configure and train the neural networks for their indeterminate parameters such as the hidden layers and their nodes, learning patterns, and training parameters.

3.1 Selection Of Data Set

The purpose of training a network is to allow it to produce accurate answers and generalize future data. The experimental data used in modeling the proposed neural model are subdivided into two groups; training and testing group. The network uses the training group to updating values of the nodes' biases and weights in order to minimize the training error. In other words, it uses this group to get the relationship between the input and output variables. While the network uses the testing group to check the generalization ability of the proposed model.

The total actual (experimental) data used in the proposed neural model are those obtained from available open literature [1, 2, 4-13, 15-18, 20, 22, 25-30, and 32-40]. A total number of (199)

beams (samples) were collected as data set. The training group must contain the extreme values of the different input parameters of the total data set. For estimating the generalization capacity of the training process, the testing set is either selected rotationally from the total data set, or is selected randomly by the computer. In this study, the testing group comprises of approximately (20)% of the collected data and is selected randomly over the entire region of data set. Accordingly, the training group is decided to comprise of (159) samples, while the testing group is comprised of (40) samples.

3.2 Defining Of Input And Output Variables

The problem's nature is the effective factor that state the defining of the input and output variables (parameters). Selection of the input variables is important to get an efficient network, while the selection of the output variables depends on what required from the network to know. In this study, the dimensions and properties of concrete and FRP bars are chosen as candidate input variables. While the output variable is only the ultimate load (P) of the considered concrete beams. For the proposed neural model, it is decided to use the following eight variables as input variables: the cross sectional width (b) of beams, cross sectional depth (h) of beams, cylinder concrete compressive strength (f'_c), cross sectional area of FRP bars (A_f), FRP bars tensile strength (f_u), FRP bars elasticity modulus (E_f), effective span length (L) of beams, and shear span ratio (m). To minimize the input variables several attempts are tried to choose their proper number to represent the properties of the considered beams. In one attempt, the gross cross sectional area of concrete is used instead of its width and depth. Also in another attempt, the reinforcement ratio of FRP bars is used as an input variable. Although good performance in training is found, but the generalization is very poor. Therefore, it is decided to use the above eight input variables for the proposed model. So, eight nodes in the input layer and (1) node in the output layer are used in the proposed neural model. The ranges of all variables are given in **Table (1)**.

3.3 Hidden Layers And Their Nodes

determining of hidden layers and their nodes depends on the network application. There is no rules available to find out their exact number. Once start with small number and then is increased until the wanted value from the model (network) is reached. This number is chosen by a trial and error process. If the nodes number is large, the operation of network will be slow and may cause overfitting in the testing group performance. And if this number is very small then the network may be unable to learn well. The suitable number will be selected by a trial and error process to get the network of the minimum error (the best performance) for both training and testing group.

Firstly, a proposed Levenberg-Marquardt back-propagation neural network is investigated with different configurations to choose the best network. Many different trial networks are trained and the optimal topology is determined by choosing the best performed network (of the less training error). Trial networks with single and multi hidden layers and nodes and with a various activation functions (hyperbolic tangent (tansig), logistic sigmoidal (logsig), and linear (purelin) function) are tested. The results show that, the (11-10) two hidden layered model gives best performance with least error in the output variable. This network, with ten nodes in the first hidden layers and twelve nodes in the second and with tansig function for hidden layers and purelin function for the output layer, gives the best performance with MSE of (0.000445) for the training group and (0.001069) for the testing group and number of epochs of (616). Thus, this configuration (topology) is adopted to the proposed network. The topology of this neural network are shown in **Figure (4)**. While the properties of this proposed model are shown in **Table (2)**.

4. Results And Discussion

A regression analysis between the obtained (predicted) results and the actual values is performed to investigate the accuracy of the proposed network. The regression coefficient of correlation (R) is used as an index in this analysis. If (R) is close to a value of one, then there is an excellent correlation between the obtained (predicted) loads and the actual loads. **Figure (5)** shows the correlation analysis of the proposed model output and the experimental values for the training group, while **Figure (6)** shows this analysis for the testing and group. From **Figure (5)**, which represents the regression analysis for the training data, the correlation coefficient (R) is (0.9988), the interception with y-axis is (0.307) and the slope is (0.997). While for the testing data, **Figure (6)**, the correlation coefficient (R) is (0.9961), interception with y-axis is (0.863) and the slope is (0.991). These analyses certify good agreement between the obtained results and the actual results.

5. Comparative Study

The proposed neural model is used to obtain and predict the ultimate load of the FRP reinforced concrete beams that used in the selected testing set of this study. A comparison between the experimental and predicted ultimate loads obtained by the proposed model (P_{ANN}) and those obtained from using the ACI 440.1R approach [3] (P_{ACI}) is presented in **Table (3)**. As can be noticed from this table, for almost specimens the proposed network gives more accurate results as compared with those predicted by the ACI 440.1R approach. The ACI 440.1R approach underestimates ultimate loads up to approximately 50% (beam number 17) and overestimates ultimate loads up to approximately 24% (beam number 27). While the proposed neural model underestimates ultimate loads up to approximately 12% (beam number 17) and overestimates ultimate loads up to approximately 8% (beam number 10).

A statistical comparison between the actual and predicted loads is also performed to check the accuracy of the proposed network and the ACI 440.1R approach of ultimate load calculation as shown in **Table (4)**. Four indices are used in this study to comparative evaluation of the behavior of the proposed network and the calculated ultimate loads using the ACI 440.1R specifications. These indices are the mean absolute error (*MAE*), root mean squared error (*RMSE*), mean absolute percentage error (*MAPE*), and fraction of variance (*FOV*). and they are given, respectively, as:

$$MAE = \frac{1}{n}\sum_{i=1}^{n}\left|u - v\right|, \qquad (2)$$

$$RMSE = \sqrt{\frac{1}{n}\sum_{i=1}^{n}(u-v)^2}\ , \qquad (3)$$

$$MAPE = \left[\frac{1}{n}\sum_{i=1}^{n}\left|(u-v)/u\right|\right]\times 100\ , \qquad (4)$$

$$FOV = 1-\sum_{i=1}^{n}(u-v)^2 \Big/ \sum_{i=1}^{n}(u-\bar{u})\ , \qquad (5)$$

where u is the actual value, v is the predicted value, $\bar{u}$ is the mean of the actual values, and n is number of specimens. If MAE is 0, RMSE is 0, MAPE is 0, and FOV is 1, then the used model will be excellent.

As can be noticed from **Table (4)**, the MAE, RMSE, MAPE, and FOV for the ultimate load prediction of the proposed neural model are (4.4, 5.7, 3.6, and 0.992), respectively. While these values for the ACI 440.1R approach are (31.4, 41.7, 21.7, and 0.582), respectively. These values proved that the proposed neural model prediction is satisfactory indicating that, an excellent agreement with the experimental data is obtained and hence the proposed network can obtain and predict loads very well and better than ACI 440.1R approach.

In **Figure (7)**, the predicted ultimate loads obtained by the proposed model (P_{ANN}) and the ACI 440.1R approach (P_{ACI}) are plotted against the actual loads. From this Figure, it is obvious that in general the ACI approach underestimates the value of the ultimate load. The coefficient of correlation R = 0.9961 and 0.7629 for P_{ANN} and P_{ACI}, respectively. These values show that the proposed neural model predicts loads much better than the ACI approach.

Therefore, with an overall average error of 3.6%, it is concluded that the developed network could be used efficiently in obtaining the ultimate loads and that the ANN provided an alternative procedure to the costly test procedures for the ultimate load prediction of FRP reinforced concrete beams.

6. Conclusions

The main important points that can be concluded from this study are as follows:

1. The artificial neural networks (ANN) have been proved its capability in predicting the ultimate load of FRP reinforced concrete beams, and it could be used this procedure as a reliable alternative to other complex or costly test procedures.

2. The proposed neural model, in the current study, has been found to be very excellent for prediction of the ultimate load of FRP reinforced concrete beams.

3. The configuration (11-10) for the proposed neural model was found to be very typical for prediction of the ultimate load of FRP reinforced concrete beams.

4. The overall average error, in ultimate load prediction, was 3.6% and 21.7% for the proposed neural model and the ACI 440.1R approach, respectively. So the proposed neural model gave more accurate results than the ACI 440.1R specifications and it could be used efficiently in predicting the ultimate load FRP reinforced concrete beams.

5. The ACI 440.1R approach was shown to give, in general, an underestimated value for the ultimate load.

References

1. **Abdalla H. A.,** 2002, "Evaluation of Deflection in Concrete Members Reinforced With Fibre Reinforced Polymer (FRP) Bars", Composite Structures, 56, P. 63–71.

2. **Abdul Hamid N. A., Thamrin R., and Ibrahim A.,** 2013, "Shear Capacity of Non-Metallic (FRP) Reinforced Concrete Beams with Stirrups", IACSIT International Journal of Engineering and Technology, Vol. 5, No. 5, P. 593-598.

3. **ACI 440.1R-06,** 2006, "Guide for the Design and Construction of Structural Concrete Reinforced with FRP Bars", American Concrete Institute.

4. **Adam M. A., Said M., Mahmoud A. A., and Shanour A. S.,** 2015, "Analytical and Experimental Flexural Behavior of Concrete Beams Reinforced With Glass Fiber Reinforced Polymers Bars", Construction and Building Materials 84, P. 354–366.

5. **Aiello M. A. and Ombres L.,** 2000, "Load-Deflection Analysis of FRP Reinforced Concrete Flexural Members", Journal of Composites for Construction, Vol. 4, No. 4, P. 164-171.

6. **AlMusallam T. H.,** 1995, "Analytical Predication of Flexural Behavior of Concrete Beams Reinforced by FRP Bars", Journal of Composites materials, Vol. 31,No.7, P. 640-657.

7. **AlSayed S. H., AlSalloum Y. A., and AlMusallam T. H.,** 2000, "Performance of Glass Fiber Reinforced Plastic Bars as a Reinforcing Material For Concrete Structures", Composites: Part B 31, P. 555-567.

8. **AlSunna R., Pilakoutas K., Hajirasouliha I., and Guadagnin M.,** 2012, "Deflection Behaviour of FRP Reinforced Concrete Beams and Slabs: An Experimental Investigation", Composites: Part B 43, P. 2125–2134.

9. **AlSunna R., Pilakoutas K., Waldron P., and AlHadeed T.,** 2006, "Deflection of FRP Reinforced Concrete Beams", Proceeding of the 2nd FIB Congress, Naples, Italy, P. 5-8.

10. **Ashour A. F.,** 2004, "Flexural and Shear Capacities of Concrete Beams Reinforced with GFRP Bars", Construction and Building Materials 20, P. 1005–1015.

11. **Ashour A. F. and Family M.,** 2006, "Tests of Concrete Flanged Beams Reinforced with CFRP Bars", Magazine of Concrete Research**,** Vol. 58, No. 9, P. 627-639.

12. **Awadallah Z. H., Ahmed M. M., Farghal O. A., and Fahmy M. F. M.,** 2014, "Some Parameters Affecting Shear Behavior of High Strength Fiber Reinforced Concrete Beams Longitudinally Reinforced with BFRP Rebars", Journal of Engineering Sciences(JES), Vol. 42, No. 5, P. 1163–1178.

13. **Barris C., Torres L. I., Turon A., Baena M., and Catalan A.,** 2009, "An Experimental Study of The Flexural Behaviour of GFRP RC Beams and Comparison with Prediction Models", Composite Structures 91, P. 286–295.

14. **Begg R., Kamruzzaman J., and Sarker R.,** 2006, "Neural Network in Healthcare: Potential and Challenges", Published in United states of Americaa by Idea Group Publishing and in United Kingdom by Idea Group Publishing, ISBN 1-59140-848-2 (hardcover)-ISBN 1-59140-849-0 (softcover).

15. **Chaallal O. and Benmokrane B.,** 1995, "Fiber Reinforced Plastic Rebars for Concrete Applications", Composites Part B 27B , P. 245 -252, 1995.

16. **Chitsazan I., Kobraei M., Jumaat M. Z., and Shafigh P.,** 2010, "An Experimental Study on the Flexural Behavior of FRP RC Beams and a Comparison of The Ultimate Moment Capacity with ACI", Journal of Civil Engineering and Construction Technology, Vol. 1 (2), P. 27-42, 2010.

17. **Duranovic N., Pilakoutas K., and Waldron P.,** 1997, "Tests on Concrete Beams Reinforced with Glass Fiber Reinforced Plastic Bars", Proceeding of the 3rd international symposium of non-metalic (FRP) reinforcement for concretestructures (FRPRCS-3), 2, p. 479-86.

18. **ElSalakawy E., Kassem C., and Benmokrane B.,** 2002, "Flexural Behaviour of Concrete Beams Reinforced with Carbon FRP Composite Bars", Montreal Quebec, Canada, P. 1-9.

19. **Graupe D.**, 2007, "Principles of Artificial Neural Networks", World Scientific Published by World Scientific Publishing Co. Pte. Ltd, Vol.6.

20. **Hamedani R. N. and Esfahani M. S.**, 2012, "Numerical Evaluation of Structural Behavior of The Simply Supported FRP RC Beams", M. Sc. Thesis, Stockholm, Sweden, P.119.

21. **Imam A., Anifowose F., and Azad A. K.,** 2014, "Residual Strength of Corroded Reinforced Concrete Beams Using an Adaptive Model Based on ANN", International Journal of Concrete Structures and Materials.

22. **Issa M. S., Metwally I. M., and Elzeiny S. M.,** 2011, "Influence of Fibers on Flexural Behavior and Ductility of Concrete Beams Reinforced With GFRP Rebars", Engineering Structures 33, P. 1754–1763, 2011.

23. **Jain R. and lee L.,** 2012, "Fiber Reinforced Polymer (FRP) Composites for Infrastructure Applications", Focusing on Innovation, Technology Implementation and Sustainability, Springer.

24. **Kamanli M., Kaltakci M. Y., Bahadir F., Balik F. S., Korkmaz H. H., Donduren M. S., and Cogurcu M. T.,** 2012, "Predicting The Flexural Behaviour of Concrete and Lightweight Concrete Beams by ANN", Indian Journal of Engineering &Materials Sciences, Vol.19, P. 87-94.

25. **Kassem C., Farghaly A. S., and Benmokrane B.,** 2011, "Evaluation of Flexural Behavior and Serviceability Performance of Concrete Beams Reinforced with FRP Bars", Journal of Composites for Construction, Vol. 15, No.5, P. 682-695.

26. **Kishi N., Mikami H., Kurihashi Y., and Sawada S.,** 2005, "Flexural Behavior of RC Beams Reinforced with AFRP Rods", Proceedings of the International Symposium on Bond Behaviour of FRP in Structures, P. 337-342.

27. **Leung H. Y. and Balendran R. V.,** 2003, "Flexural Behaviour of Concrete Beams Internally Reinforced with GFRP Rods and Steel Rebars", Structural Survey, Vol. 21, No. 4, P. 146-157.

28. **Park Y., Kim Y. H., and Lee S. H.,** 2014, "Long-Term Flexural Behaviors of GFRP Reinforced Concrete Beams Exposed to Accelerated Aging Exposure Conditions", Polymers , Vol. 6, P. 1773-1793.

29. **Pecce M., Manfredi G., and Cosenza E.,** 2000, "Experimental Response and Code Models of GFRP RC Beams in Bending", Journal of Composites for Construction, Vol. 4, No. 4, P.182-190.

30. **Rafi M. M., Nadjai A., Ali F., and Talamona D.,** 2006, "Aspects of Behaviour of CFRP Reinforced Concrete Beams in Bending", Construction and Building Materials 22, P. 277–285.

31. **Raheman A. and Modani P. O.**, 2013, "Prediction of Properties of Self Compacting Concrete Using Artificial Neural Network", International Journal of Engineering Research and Applications (IJERA), Vol. 3, No. 4, P. 333-339.

32. **Rahgozar R., Ghalehnovi M., and Adili E.,** 2009, "Comparing The Behavior of Reinforced HSC Beams with AFRP Bars and Confined HSC Beams With AFRP Sheets Under Bending", Taylor & Francis Group, P.1231- 1236.

33. **Rasheed H. A., Nayal R., and Melhem H.,** 2004, "Response Prediction of Concrete Beams Reinforced With FRP Bars", Composite Structures, 65, P. 193–204.

34. **Saikia B., Kumar P., Thomas J., Rao K. S. N., and Ramaswamy A.**, 2007, "Strength and Serviceability Performance of Beams Reinforced with GFRP Bars in Flexure", Construction and Building Materials, 21 , P. 1709–1719.

35. **Shin S., Seo D., and Han B.,** 2009, "Performance of Concrete Beams Reinforced with GFRP Bars", Journal of Asian Architecture and Building Engineering, Vol. 8, No.1, P. 197-203.

36. **Tomlinson D. and Fam A.,** 2014, "Performance of Concrete Beams Reinforced with Basalt FRP for Flexure and Shear", Journal of Composites for Construction,19, P. 04014036-1-04014036-10.

37. **Wang H. and Belarbi A.,** 2011, "Ductility Characteristics of Fiber-Reinforced-Concrete Beams Reinforced with FRP Rebars", Construction and Building Materials, 25, P. 2391–2401.

38. **Yost J. R., Goodspeed C. H., and Schmeckpeper E. R.,** 2001, "Flexural Performance of Concrete Beams Reinforced With FRP Grids", Journal of Composites for Construction, Vol. 5, No. 1, P. 18-25.

39. **Yuan F.**, **Pan J., and Leung C. K. Y.,** 2013, "Flexural Behaviors of ECC and Concrete/ECC Composite Beams Reinforced with Basalt Fiber Reinforced Polymer", Journal of Composites for Construction , Vol, 17, No. 5, P. 591-602.

40. **Zhang L., Sun Y., and Xiong W.,** 2014, "Experimental Study on The Flexural Deflections of Concrete Beam Reinforced with Basalt FRP Bars", Materials and Structures.

Table (1) Input And Output Variables

Variable	**Range**
Input variables:	
Width of beam, *b,* (mm)	80 – 500
Depth of beam, *h,* (mm)	100 – 590
Concrete compressive strength, f'_c, (MPa)	13.7 – 85.6
Area of FRP bars, A_f, (mm^2)	39.3 – 19635
FRP bars tensile strength, f_u, (MPa)	126.2 – 2250
FRP bars elasticity modulus, E_f, (MPa)	30000 – 200000
Length of beam, *L,* (mm)	400 – 4200
Shear span ratio, *m*	0.273 – 0.47
Output variable:	
Ultimate load, *P,* (kN)	16 – 365.4

Table (2) Properties Of The Proposed Neural Model

Network	***Nodes in 1st hidden layer***	***Nodes in 2nd hidden layer***	***Nodes in output layer***	***Epochs***	***MSE for training set***	***MSE for testing set***
11 – 10	11	10	1	616	0.000445	0.001069

Table (3) Actual And Predicted Ultimate Load

Beam No.	***Type of FRP bars***	***Concrete Compressive Strength, f'c (MPa)***	***FRP reinforcement ratio to balanced ratio, (e_f / e_{bf})***	***Ultimate load (kN)***			P_{ANN}/P_{EXP}	P_{ACI}/P_{EXP}
				Actual P_{EXP}	***Predicted***			
					By	***By***		

					ANN P_{ANN}	*ACI* P_{ACI}		
1	GFRP	24.5	2.67	75.2	74.2	42.5	0.987	0.565
2	GFRP	30.0	1.99	96.0	96.3	79.2	1.003	0.825
3	GFRP	27.6	0.42	33.7	33.9	31.6	1.006	0.938
4	GFRP	27.6	0.69	51.2	53.4	62.5	1.043	1.221
5	GFRP	38	4.05	40.7	40.5	34.7	0.995	0.853
6	GFRP	27.6	4.30	41.6	41.2	33.4	0.990	0.803
7	GFRP	27.6	3.44	127.4	118.6	75.4	0.931	0.592
8	GFRP	59.8	3.68	143.4	150.2	89.5	1.047	0.624
9	GFRP	56.3	5.58	169.8	164.6	102.8	0.969	0.605
10	GFRP	55.2	4.43	85.1	92.3	55.7	1.085	0.655
11	GFRP	39.6	3.38	134.9	140.5	82.2	1.042	0.609
12	BFRP	61.7	3.23	200.0	209.8	164.1	1.049	0.821
13	CFRP	40.1	1.76	170.5	162.7	162.0	0.954	0.950
14	CFRP	40.4	2.52	178.7	180.0	158.2	1.007	0.885
15	GFRP	39.3	3.36	162.3	161.9	127.4	0.998	0.785
16	GFRP	32.5	1.19	185.5	187.3	211.7	1.010	1.141
17	GFRP	41.4	1.28	154.1	134.9	77.9	0.875	0.506
18	GFRP	41.4	1.71	106.4	100.9	55.4	0.948	0.521
19	GFRP	29.8	1.67	80.0	76.0	70.0	0.950	0.875
20	GFRP	29.8	6.26	118.0	110.0	117.8	0.932	0.998
21	CFRP	29.8	0.76	76.0	74.0	63.8	0.974	0.839
22	CFRP	29.8	1.14	105.0	100.0	100.5	0.952	0.957
23	CFRP	29.8	1.81	125.0	123.0	117.2	0.984	0.938
24	GFRP	40.6	1.09	76.0	80.0	79.7	1.053	1.048
25	GFRP	40.0	5.74	112.0	118.0	138.4	1.054	1.236
26	CFRP	47.0	0.67	70.0	75.0	75.5	1.071	1.079
27	CFRP	44.7	1.34	100.0	101.0	124.4	1.010	1.244
28	CFRP	44.0	3.18	120.0	125.0	145.1	1.042	1.209
29	GFRP	30.0	3.61	123.2	127.8	129.1	1.037	1.048
30	CFRP	30.0	3.13	135.0	139.9	132.3	1.036	0.980
31	GFRP	48.0	4.89	135.0	130.7	104.3	0.968	0.773
32	GFRP	48.0	4.80	138.6	134.6	119.9	0.971	0.865
33	CFRP	48.0	4.25	155.0	144.8	107.3	0.934	0.692
34	GFRP	24.0	1.21	92.8	99.0	79.6	1.067	0.858
35	GFRP	24.0	1.82	125.6	132.1	93.2	1.052	0.742

36	GFRP	29.3	1.06	207.0	209.5	137.1	1.012	0.662
37	GFRP	29.3	2.28	307.0	302.7	192.6	0.986	0.627
38	GFRP	29.9	2.44	229.7	228.0	162.7	0.993	0.708
39	GFRP	36.5	2.12	227.0	228.0	177.4	1.004	0.781
40	GFRP	29.9	5.12	331.3	332.8	230.9	1.005	0.697
Average							1.001	0.844
Standard deviation							0.007	0.032

Table (4) Statistical comparison

Norm	***Proposed neural model (NN1)***	***ACI approach***
Mean absolute error (MAE)	4.4	31.4
Root mean squared error (RMSE)	5.7	41.7
Mean absolute percentage error (MAPE)	3.6	21.7
Fraction of variance (FOV)	0.992	0.582

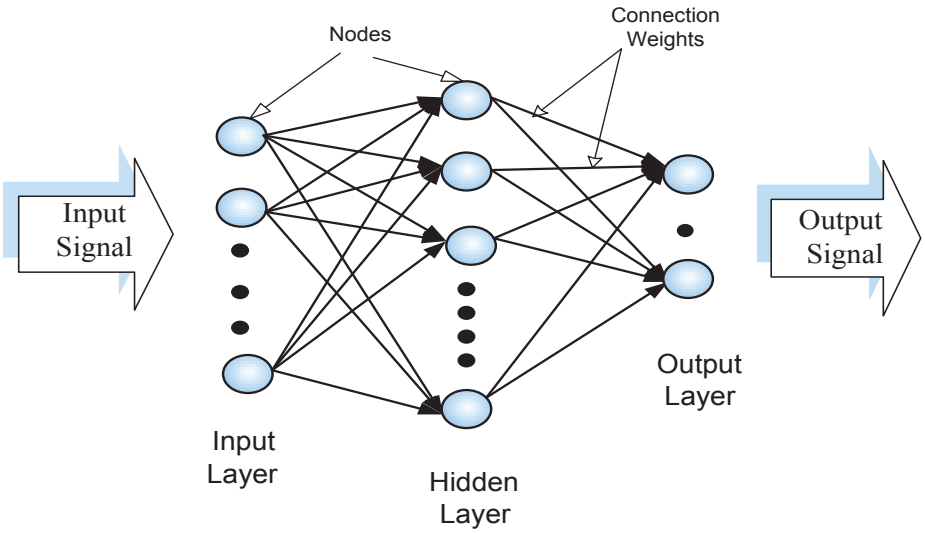

Figure (1) Architecture Of A Neural Network

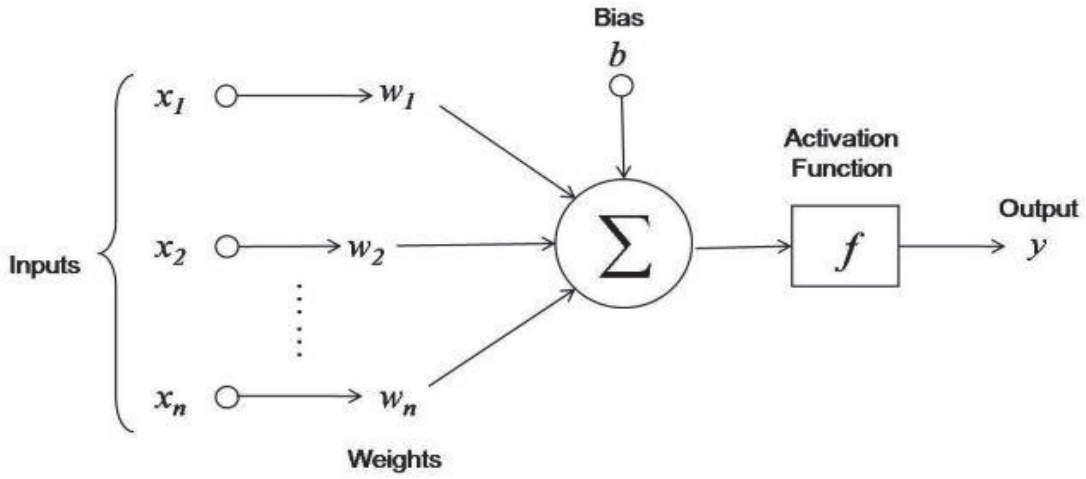

Figure (2) Artificial Neuron Model

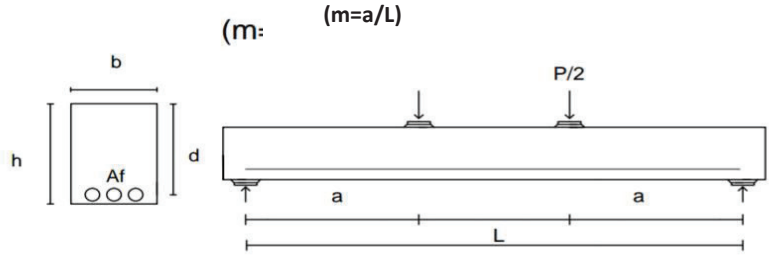

Figure (3) Four Point Loading Beam

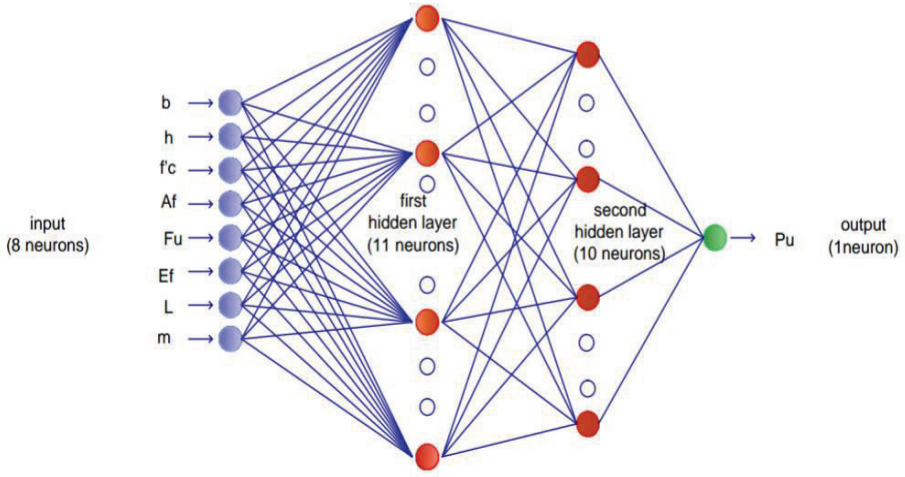

Figure (4) Proposed Neural Model Topology

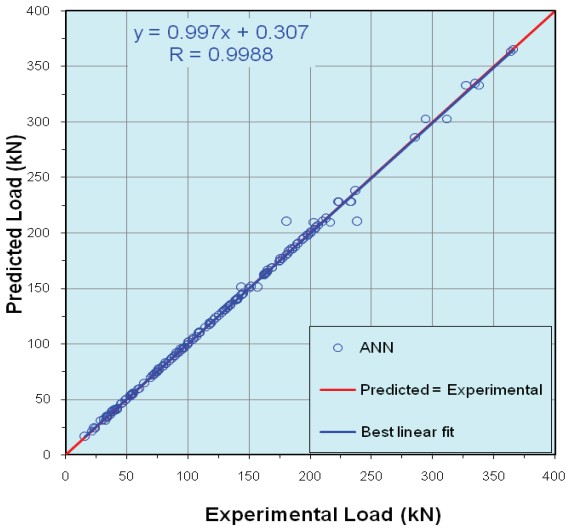

Figure (5) Regression Analysis For Training Group

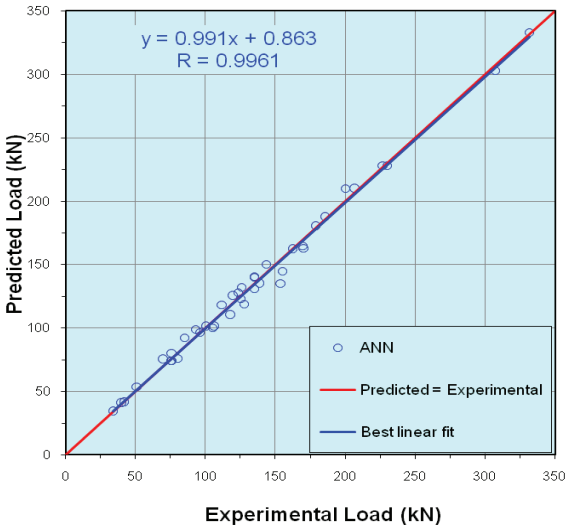

Figure (6) Regression Analysis For Testing Group

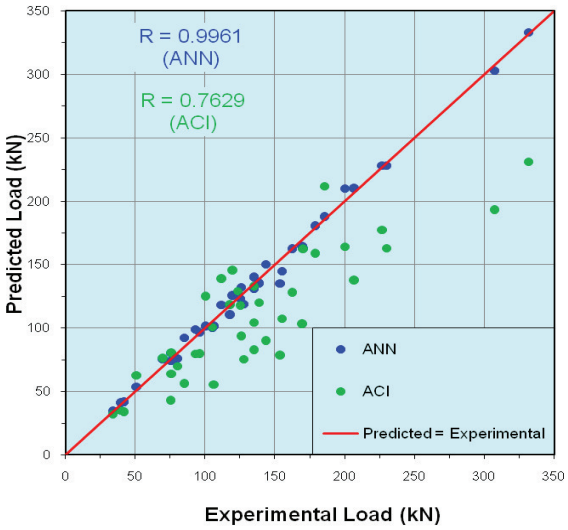

Figure (7) Comparison Between Predicted And Actual Loads